Redox Biology 19 (2018) 134–146

Contents lists available at ScienceDirect

Redox Biology

journal homepage: www.elsevier.com/locate/redox

Over-expression of a cardiac-specific human dopamine D5 receptor mutation in mice causes a dilated cardiomyopathy through ROS over-generation by NADPH oxidase activation and Nrf2 degradation

Xiaoliang Jiang[a,1], Yunpeng Liu[a,1], Xing Liu[a], Wenjie Wang[a], Zihao Wang[a], Yongyan Hu[a], Yuanyuan Zhang[a], Yanrong Zhang[a], Pedro A. Jose[c,d], Qiang Wei[a,b,*], Zhiwei Yang[a,b,*]

[a] Institute of Laboratory Animal Science, Chinese Academy of Medical Sciences (CAMS) & Comparative Medicine Centre, Peking Union Medical Collage (PUMC), 5 Pan Jia Yuan Nan Li, Chaoyang District, Beijing 100021, PR China
[b] Beijing Collaborative Innovation Center for Cardiovascular Disorders, 5 Pan Jia Yuan Nan Li, Chaoyang District, Beijing 100021, PR China
[c] Department of Medicine, Division of Kidney Diseases & Hypertension, The George Washington University School of Medicine & Health Sciences, Washington, DC 20052, USA
[d] Department of Pharmacology and Physiology, The George Washington University School of Medicine & Health Sciences, Washington, DC 20052, USA

ARTICLE INFO

Keywords:
Dilated cardiomyopathy (DCM)
Dopamine D5 receptor (D5R)
Reactive oxygen species (ROS)
Nrf2

ABSTRACT

Dilated cardiomyopathy (DCM) is a severe disorder caused by medications or genetic mutations. D_5 dopamine receptor (D5R) gene knockout ($D5^{-/-}$) mice have cardiac hypertrophy and high blood pressure. To investigate the role and mechanism by which the D5R regulates cardiac function, we generated cardiac-specific human D5R F173L($hD5^{F173L}$-TG) and cardiac-specific human D5R wild-type ($hD5^{WT}$-TG) transgenic mice, and H9c2 cells stably expressing $hD5^{F173L}$ and $hD5^{WT}$. We found that cardiac-specific $hD5^{F173L}$-TG mice, relative to $hD5^{WT}$-TG mice, presented with DCM and increased cardiac expression of cardiac injury markers, NADPH oxidase activity, Nrf2 degradation, and activated ERK1/2/JNK pathway. H9c2-$hD5^{F173L}$ cells also had an increase in NADPH oxidase activity, Nrf2 degradation, and phospho-JNK (p-JNK) expression. A Nrf2 inhibitor also increased p-JNK expression in H9c2-$hD5^{F173L}$ cells but not in H9c2-$hD5^{WT}$ cells. We suggest that the D5R may play an important role in the preservation of normal heart function by inhibiting the production of reactive oxygen species, via inhibition of NADPH oxidase, Nrf2 degradation, and ERK1/2/JNK pathways.

1. Introduction

Dilated cardiomyopathy (DCM) is a severe disorder caused by ventricular dilatation and cardiac dysfunction in response to inflammatory, metabolic, and toxic effects of medications or genetic mutations [1–4]. Despite the many causes of DCM, there are many similarities in the final structural and functional alterations, related to long-term stress and neurohormonal activation [5], that eventually lead to systolic heart failure. Increased left ventricular end-diastolic volume and decreased left ventricular ejection fraction are risk factors for cardiac morbidity and mortality in the general population [6]. The mechanisms that determine the progression of DCM are not completely understood, but 30–48% are related to genetic mutations [1–4]; DCM is also closely associated with hypertension [3].

We have reported that the global disruption of the D5 receptor (D5R) gene ($D5^{-/-}$), one of the two D1-like dopamine receptors, in mice causes high blood pressure [7,8]. The $D5^{-/-}$ mice also have cardiac hypertrophy and increased heart weight [8]. Humans have single nucleotide polymorphisms in the D5R gene that are associated with diminished D5R function [9]. The mutant human D5R F173L is associated with decreased D5R function and transgenic (TG) mice globally expressing the human $D5^{F173L}$ ($hD5^{F173L}$) have high blood pressure [10]. Global $hD5^{F173L}$-TG mice present with cardiac hypertrophy at five months of age (unpublished data), presumably secondary to increased blood pressure, similar to that observed in $D5^{-/-}$ mice after two months of age [8].

The elevated blood pressure in $D5^{-/-}$ mice is related to increased oxidative stress, due in part to increased renal NADPH oxidase activity and decreased HO-1 activity [7,11]. Renal NADPH oxidase activity is also increased in global $hD5^{F173L}$-TG mice [10]. Therefore, we

* Corresponding authors at: Institute of Laboratory Animal Science, Chinese Academy of Medical Sciences (CAMS) & Peking Union Medical Collage (PUMC), 5 Pan Jia Yuan Nan Li, Chaoyang District, Beijing 100021, PR China.
E-mail addresses: weiqiang0430@cnilas.org (Q. Wei), yangzhiwei@cnilas.pumc.edu.cn (Z. Yang).
[1] These authors contributed equally to this work.

https://doi.org/10.1016/j.redox.2018.07.008
Received 28 June 2018; Received in revised form 10 July 2018; Accepted 12 July 2018
Available online 17 July 2018
2213-2317/ © 2018 The Authors. Published by Elsevier B.V. This is an open access article under the CC BY-NC-ND license (http://creativecommons.org/licenses/BY-NC-ND/4.0/).

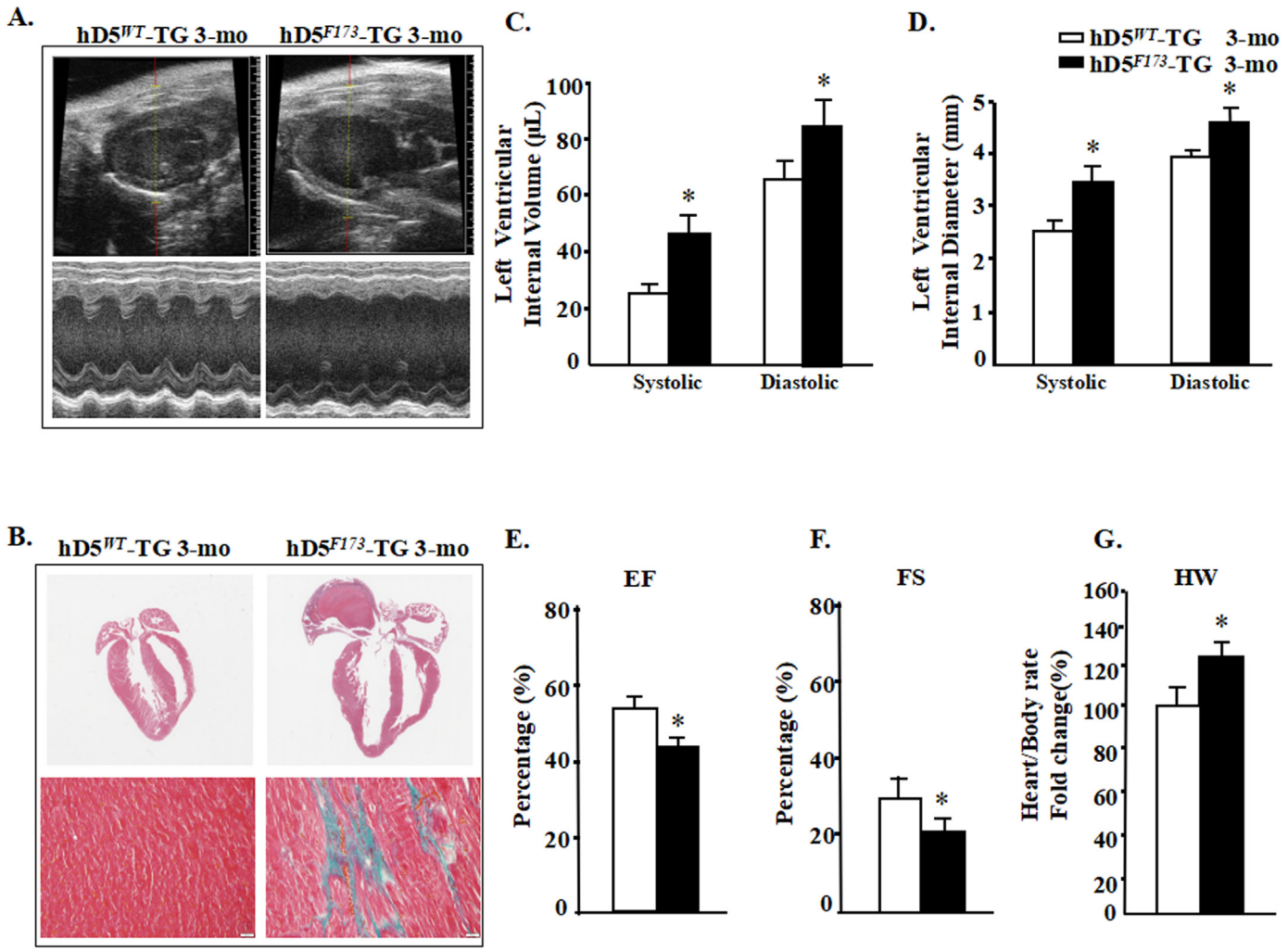

Fig. 1. D5R functional deficiency produces dilated cardiomyopathy. A: Representative echocardiograms from cardiac-specific hD5^{WT}-TG and hD5^{F173L}-TG mice. **B:** Cardiac sections stained with H&E (top) and Masson's trichrome stain (bottom) from 3-month-old mice. Scale bar: 5 μm. **C–G:** Echocardiographic analysis of cardiac volume and function (n = 12 mice/group); *P < 0.05 vs. D5^{WT}-TG. EF = ejection fraction, FS = fractional shortening, HW = heart weight.

hypothesized that the D5R may directly regulate cardiac remodeling and function by inhibition of NADPH oxidase activity and stimulation of antioxidants, including HO-1. The D1R, unlike the D5R, has not been reported to affect HO-1 expression or function [12]. Nuclear factor E2-related factor 2 (Nrf2), which is an important positive regulator of antioxidant genes, has been reported to preserve the function of the D1R, the other D1-like receptor, in the presence of oxidative stress [13]. Therefore, we studied in vivo the role of NADPH oxidase and Nrf2 on pathways related to cardiac function in transgenic mice expressing human D5^{F173L} or human D5^{WT} only in the myocardium, cardiac specific hD5^{F173L}-TG and hD5^{WT}-TG mice, which endogenous D5R expression in heart was prevented. We determined further the role of Nrf2 and related pathways on oxidative stress in a rat cardiomyoblast cell line (H9c2) [14], heterologously expressing hD5^{F173L} (H9c2-hD5^{F173L}) or hD5^{WT} (H9c2-hD5^{WT}).

2. Methods

2.1. Materials

An immortalized rat heart cell line (H9c2 cell) was obtained from the Chinese Academy of Sciences for Type Culture Collection, Shanghai, China. Adult (2-month old) male C57Bl/6J mice were bought from Beijing HFK Bioscience Co, LTD. All animal-related studies were approved by the Institutional Animal Care and Use Committee of the Institute of Laboratory Animal Science, Peking Union Medical College, China, and the animals were handled according to the guiding principles published in the National Institutes of Health Guide for the Care and Use of Laboratory Animals.

2.2. hD5^{WT} and hD5^{F173L} cell transfections

The full-length hD5^{WT} or hD5^{F173L} cDNA, subcloned into a pcDNA6/V_5-His vector between the *Eco*RI and Xbal sites, was transfected into H9c2 cells [14], using LT1 transfection reagents. The successful transfection of hD5R cDNA was verified by immunoblotting for His/V_5 expression and RT-PCR. Empty vector-transfected H9c2 cells served as negative controls.

2.3. Cell culture and drug treatment

H9c2-hD5^{F173L} and H9c2-hD5^{WT} cells were cultured in DMEM containing 10% fetal bovine serum (FBS), 1% penicillin, and 1% streptomycin in an incubator with a temperature set at 37 °C and 5% CO_2 atmosphere. When the cells were 90–95% confluent, they were serum-starved for 2 h, and treated for 1 h in serum-free medium with phosphate-buffered saline (PBS), 1 μM ML385 (Nrf2 inhibitor)[15], or 10 μM SP600125 (JNK inhibitor)[16].

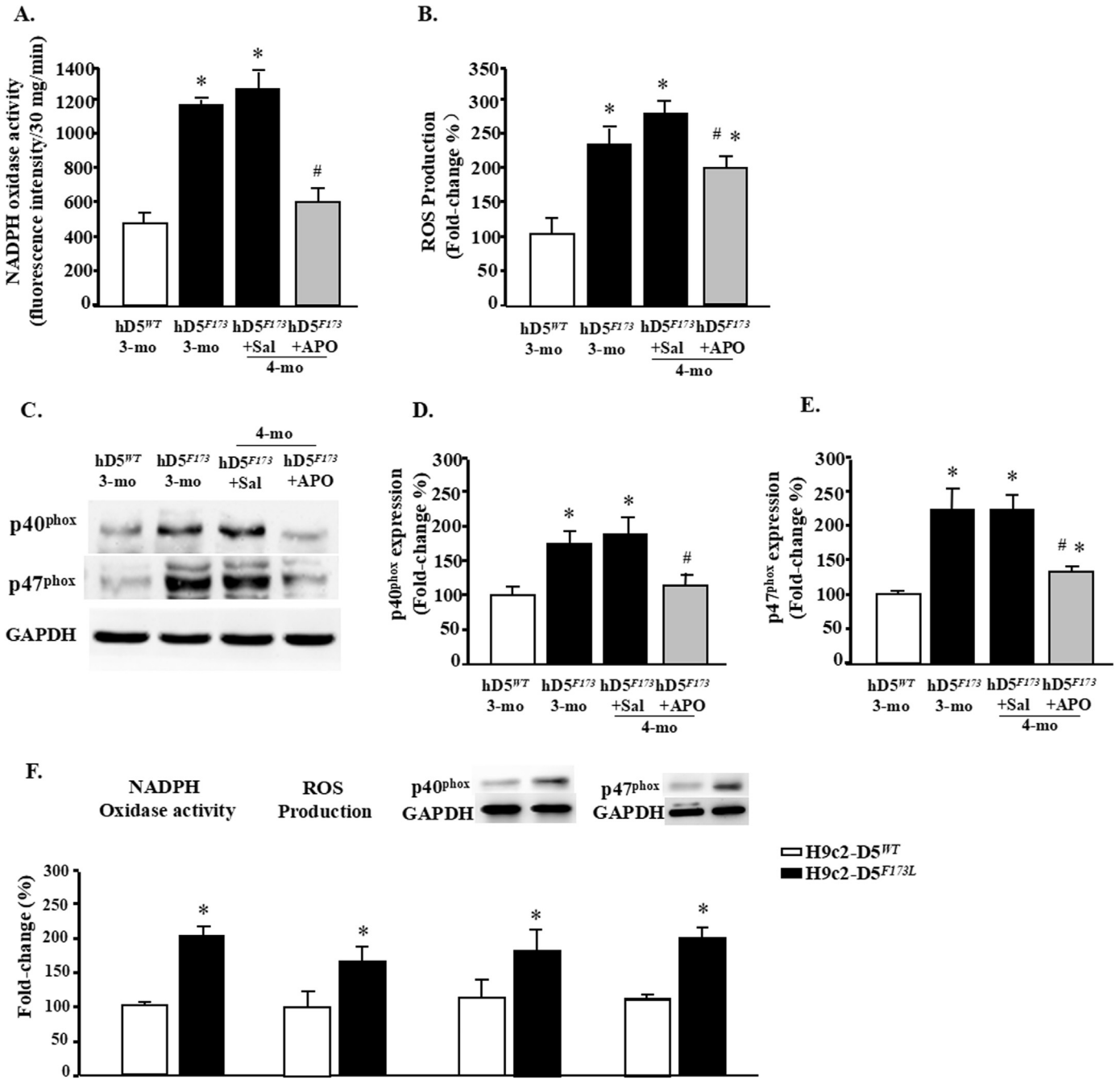

Fig. 2. D5R functional deficiency increases myocardial oxidative stress. Plasma membrane proteins were extracted from hearts of 3-month-old cardiac-specific human $D5^{WT}$-TG ($hD5^{WT}$) and $hD5^{F173L}$-TG mice ($hD5^{F173}$) and 4-month-old cardiac-specific $hD5^{F173}$ mice treated with saline ($hD5^{F173}$ + Sal) or apocynin ($hD5^{F173}$ + APO, 1 mmol/kg/day) for 4 weeks, starting at 3 months of age (n = 12 mice/group, regardless of age). **A** and **F:** NADPH oxidase activity was quantified by lucigenin chemiluminescence assay. *P < 0.05 vs. $hD5^{WT}$ mice; #P < 0.05 vs. $hD5^{F173L}$ + Sal. **B** and **F:** ROS production was quantified by H_2DCF-DA. *P < 0.05 vs. $hD5^{WT}$ mice; #P < 0.05 vs. $hD5^{F173L}$ + Sal. **C–E:** p40phox and p47phox expression was semiquantified by western blot. *P < 0.05 vs. $hD5^{WT}$-TG mice; #P < 0.05 vs. $hD5^{F173L}$ + Sal. **F:** NADPH oxidase activity, ROS production, and p40phox and p47phox protein expression were quantified in H9c2-$D5^{WT}$ and H9c2-$D5^{F173L}$ cells. *P < 0.05 vs. H9c2-$D5^{WT}$ cells (n = 8/group).

2.4. Cardiac-specific transgenic (TG) mice and drug administration

Cardiac-specific $hD5^{F173}$-TG and $hD5^{WT}$-TG mice were generated from C57Bl/6J mice, according to the following procedures. The full-length $hD5^{WT}$ or $hD5^{F173L}$ cDNA was subcloned into an expression plasmid under the α-myosin heavy chain (α-MHC) promoter. The TG mice were generated by the oocyte microinjection method [10]. The genotype of the TG mice was verified by polymerase chain reaction, using the primers 5′GGACCGCTACTGGGCCATCT and 5′GGGTCTTGA GAACCTTGGTC, and analysis of the sequence of the amplified 488 base-pair fragment of the hD5R gene.

To determine the role of NADPH oxidase in the pathogenesis of DCM in $hD5^{F173L}$-TG mice, we studied the effect of apocynin, a drug that inhibits NADPH oxidase activity by impeding the assembly of the $p47^{phox}$ and $p67^{phox}$ subunits into the NADPH oxidase complex at the plasma membrane [7,17–19]. At 3 months of age, F0 generation of $hD5^{F173L}$-TG and $hD5^{WT}$-TG mice were injected intraperitoneally, daily for four weeks, with apocynin (1 mmol/kg/day, Sigma), or PBS

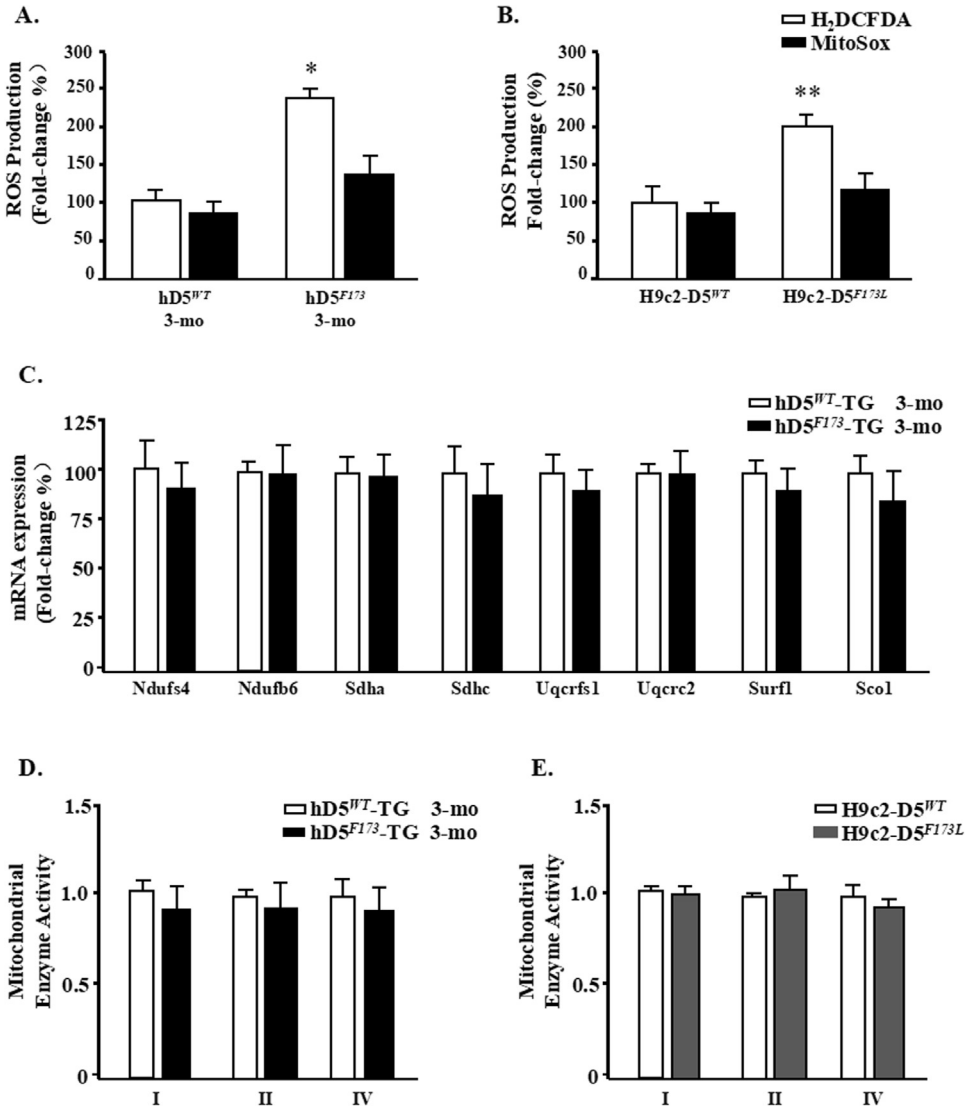

Fig. 3. Mitochondrial ROS and assessment in cardiac-specific hD5^{F173}-TG mice. Temporal analysis of ROS levels in **(A)** D5R^{WT}-TG and D5R^{F173L}-TG mice (3 months) or in **(B)** H9c2-hD5^{F173L} and H9c2-hD5^{WT} cells. ROS levels were measured at the indicated time points by incubating with H_2DCF-DA (total intracellular ROS) or MitoSox fluorescent probes (mitochondrial ROS). *p < 0.05 vs. D5R^{WT}-TG mice (n = 7), **p < 0.05 vs. H9c2-hD5^{WT} cells (n = 5). **C:** Fold changes of sub-mitochondrial particles gene expression in D5R^{F173L}-TG mice relative to D5R^{WT}-TG mice (n = 7). Fold changes of Complex I, II and IV enzyme activities for **(D)** in vivo study (n = 7) and **(E)** in vitro study (n = 5).

(0.1–0.3 ml), as a control. Thereafter, echocardiographic examinations were performed weekly, as described below. At the end of the 4-week treatment, the mice were weighed and anesthetized (2.5% Avertin, 0.012 ml/g body weight) and the hearts were harvested, weighed, and subjected to studies, as described below.

2.5. Echocardiography

The mice, anesthetized by the intraperitoneal injection of 2.5% Avertin (as indicated above), were placed on a warm pad to keep the rectal temperature around 37 °C. The chests were shaved and covered with warm echocardiography gel. The heart rate, about 400–500 beats per minute, was monitored. The hearts were imaged with a 30 MHz linear transducer (VisualSonics Vevo 770), with the mouse at a shallow left-side position. Two-dimensional left ventricular (LV) echocardiograms were obtained by placing the transducer along the long-axis of the LV, and directed to the right side of the neck of the mouse. Then, the transducers were rotated 90° clockwise and the LV short-axis views were visualized. The images showing the positions and directions of the transducer for basic mouse echocardiography views are shown in Fig. 1**A.** Two D-guided LV M-modes at the papillary muscle level were recorded from either the short-axis and long-axis views. Doppler wave forms from other regions of the heart were recorded, as needed.

2.6. NADPH oxidase activity

Cardiac membranes were prepared by a membrane and cytoplasmic protein extraction kit (Sangon Biotech, Shanghai). NADPH oxidase activity (light units per g protein per minute) of cardiac membranes was measured by NADPH-induced chemiluminescence with 5 μmol/L lucigenin and 100 μmol/L NADPH [7,11]. The specificity of the NADPH-dependent O_2^- production was verified by treatment with the flavoprotein inhibitor diphenyleneiodonium (DPI).

2.7. Intracellular ROS and mitochondrial ROS measurement

Intracellular ROS were analyzed using hydro-dichlorofluorescein diacetate (H_2DCF-DA) (Life technologies) as probes. Post-treatment, H9c2 cells or heart homogenate were collected and incubated with 100 mM Mito-tracker Red FM/ H_2DCF-DA (dissolved in DMSO) for 30 min at 37 °C. Cells were then washed three times with PBS and the intracellular accumulation of fluorescent DCF-DA was measured by fluorescence microplate (Carl Zeiss MicroImaging, NY).

For mitochondrial ROS, isolated mitochondria were loaded with MitoSOX red (5 μM, for 10 min) according to the manufacturer's instruction. Sequential 2-D confocal images were taken at 405 nm excitation, and emission was collected at > 560 nm. To calculate the rate of MitoSOX signal change (dF/dt), fluorescent signals during a 5-min

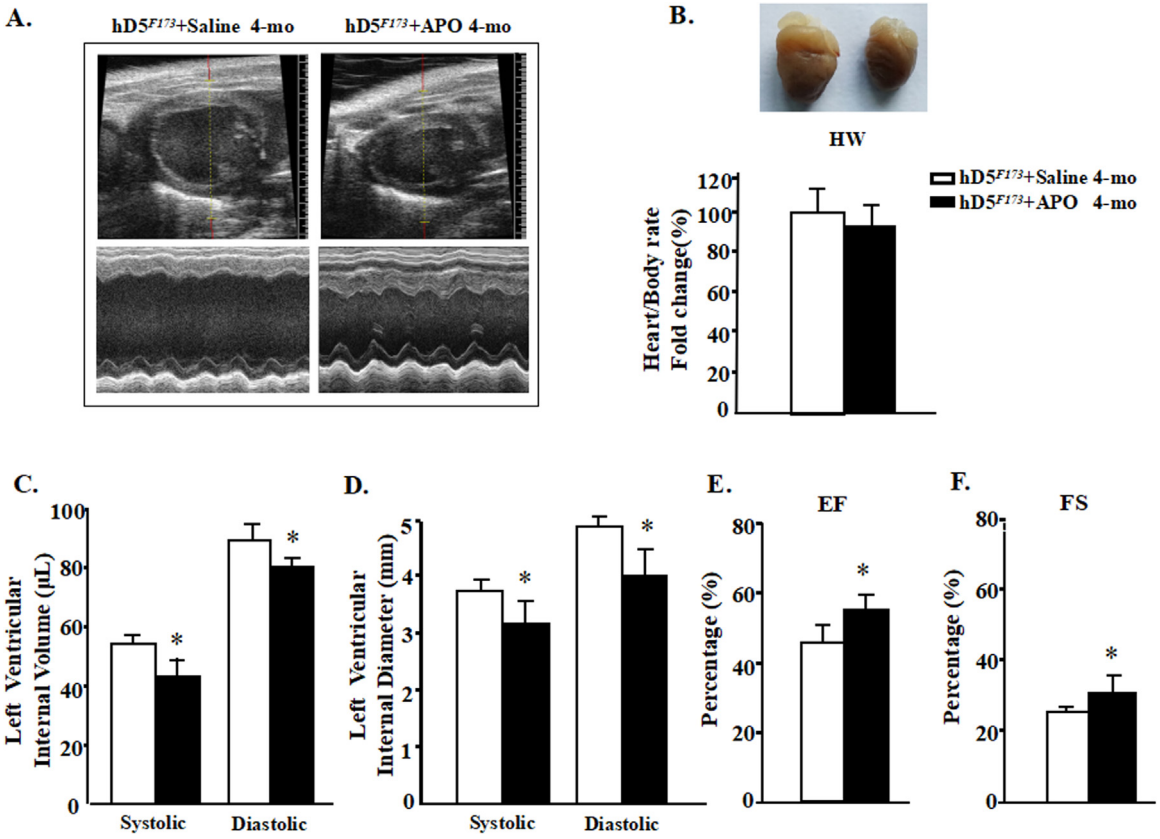

Fig. 4. Apocynin prevents the cardiac enlargement and improves cardiac function in cardiac cardiac-specific hD5^{F173}-TG mice (hD5^{F173L}). A: Representative echocardiograms of 4-month-old cardiac-specific hD5^{F173L}-TG mice treated with saline (hD5^{F173L} + Saline) or apocynin (APO, 1 mmol/kg/day) (hD5^{F173L} + APO) for 4 weeks, starting at 3 months of age (n = 10 mice/group). **B:** Heart size and weight. **C–F:** Echocardiographic analysis of cardiac volume and function. (n = 10 mice/group); *P < 0.05 vs. hD5^{F173} + Saline. EF = ejection fraction, FS = fractional shortening.

period before [20].

2.8. Mitochondrial isolation and Enzyme activity

Heart mitochondria were isolated from the rest of the homogenatesas previously described [21]. In brief: Whole heart were placed in ice cold isolation medium (250 mM Sucrose, 10 mM Tris, 0.5 mM EDTA pH 7.4 at 4 °C) immediately after killing the mice, and transferred to the Dounce glass tissue grinder to homogenise. An aliquot of the homogenates was immediately snap frozen and stored at − 70 °C.

The mitochondrial membrane potential was measured by JC-1 staining (T3168, Life technologies) After incubation with JC-1 dye, fluorescence at 485 nm was measured by a fluorometer (BioTek, Winooski, VT) according to the manufacturer's instruction [22].

2.9. Histopathology

After the mice were euthanized with an overdose of pentobarbital, The anesthetized mice was exposured to the heart and cut at auricle. The heart was perfused with HTK solution 4 °C via the tip of heart at a constant perfusion pressure of 80 ± 2 mmHg using a peristaltic pump (Gilson Minipuls 4, Middleton, WI, USA). [K^+] concentration in HTK solution is 9 mmol/L, low potassium can avoid the injury of high concentration of potassium on myocardium and coronary artery endothelium and make cardiac arrest during diastolic phase [23]. Then the heart was perfused in 10% formalin, and harvest. The whole heart was fixed in 10% formalin. The fixed hearts was embedded in paraffin, and then cut serially from the apex to the base. The sections were stained with hematoxylin-eosin and Masson's trichrome for histopathological analyses. Images of transverse sections were captured digitally, and the cardiomyocyte cross-sectional areas were measured using a Scion imaging system (Scion, Frederick, MD) [24,25]. The outlines of at least 200 cardiomyocytes in each section were traced and the data were averaged. To assess the degree of fibrosis using Masson's trichrome stain, the images from at least 10 fields for each heart were analyzed, as described previously [25,26].

2.10. Immunoblotting

Mouse cardiac plasma membranes and homogenates and H9c2 cell lysates were prepared for immunoblotting, as previously reported [7,10,11]. The samples were immunoblotted with well characterized anti-p40^{phox} (1:500, Epitomics), anti-p47^{phox} (1:1000, Epitomics), anti-Nrf2 (1:1000, Abcam), anti-P84 (1:500, Abcam), anti-phospho ERK1/2 (p-ERK1/2), anti-phospho JNK (p-JNK), anti-phospho P38 (p-P38), anti-ERK1/2, and anti-JNK, anti-P38 (1:1000, Cell Signaling Technology) antibodies. Uniformity of protein loading and membrane transfer was determined by immunoblotting for GAPDH.

2.11. Quantitative real-time PCR

Total RNA was purified using the RNeasy RNA Extraction Mini kit (Qiagen, Valencia, CA). RNA samples were converted into first strand cDNA using an RT2 First Strand kit, following the manufacturer's protocol (Qiagen). Quantitative gene expression was analyzed by real-time PCR, performed on an ABI Prism 7900 HT (Applied Biosystems, Foster City, CA). The assay used gene specific primers (Qiagen) and SYBR Green real-time PCR detection method (Qiagen) and was performed as described in the manufacturer's manual. Primers used were as Supplementary Table 1. Data were analyzed using the ΔΔCt method [27].

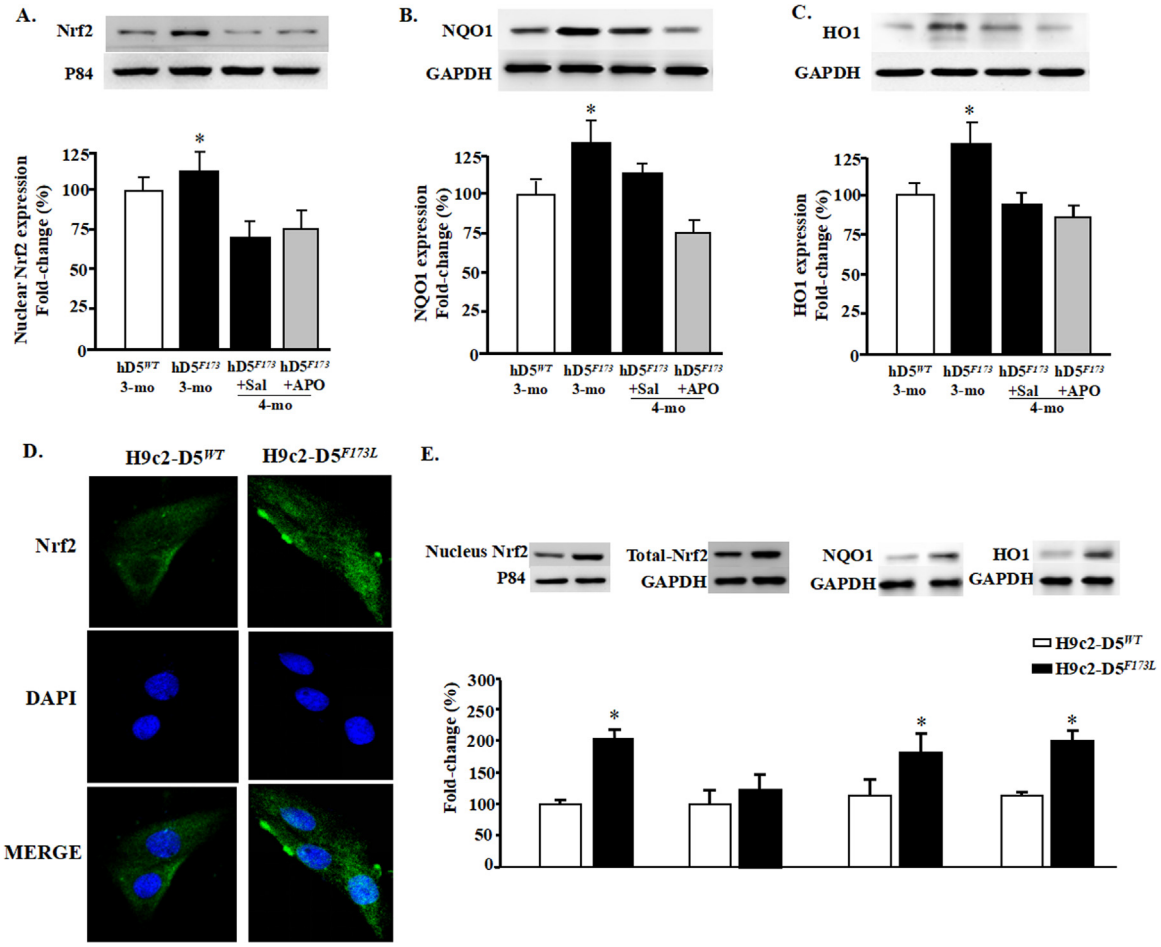

Fig. 5. D5R functional deficiency impairs nuclear Nrf2 translocation and downstream pathway. A: Nuclear proteins were extracted from the hearts of 3-month-old cardiac-specific human D5^{WT}-TG (hD5^{WT}) and hD5^{F173L}-TG (hD5^{F173}) mice and 4-month-old cardiac-specific hD5^{F173} mice treated with saline (hD5^{F173} + Sal) or apocynin (hD5^{F173} + APO, 1 mmol/kg/day) for 4 weeks, starting at 3 months of age (n = 12 mice/group). Nrf2 and P84 (nucleus marker) were semi-quantified by western blot. **B:** and **C**: NQO1 and HO1 expression was semiquantified by western blot. *P < 0.05 vs. hD5^{WT} mice (3-month-old). **D:** Nrf2 location in H9c2-D5^{WT} and H9c2-D5^{F173L} cells was determined by immunofluorescence. Green: Nrf2 Blue: DAPI. **E**: Protein expressions of Nrf2, NQO1, and HO1 were quantified by western blotting in H9c2 cells. *P < 0.05 vs. H9c2-D5^{WT} cells (n = 8 /group).

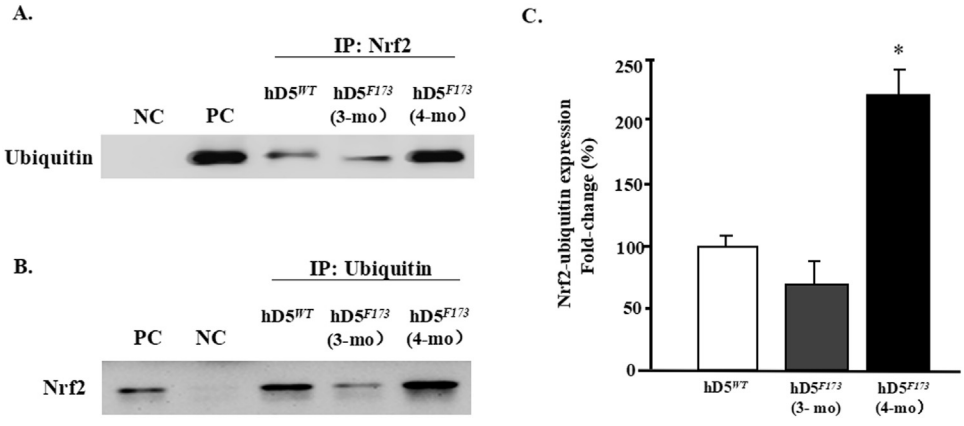

Fig. 6. Nrf2 ubiquitination in hD5^{F173L} mice. A: Total heart lysates from cardiac-specific hD5^{WT}- and hD5^{F173L}-TG mice (3- and 4-month-old) were immunoprecipitated with anti-Nrf2 antibody and immunoblotted with anti-ubiquitin antibody. **B:** Total heart lysates from cardiac-specific D5^{WT}- and hD5^{F173L}-TG mice (3- and 4-month-old) were immunoprecipitated with anti-ubiquitin antibody and immunoblotted with anti-Nrf2 antibody. **C:** Data are expressed as mean ± S.E. n = 4mice/group.*P < 0.05 vs. others, one-way ANOVA, Holm-Sidak test, NC = negative control, PC = positive control.

2.12. Co-immunoprecipitation

Co-immunoprecipitation was performed using an immunoprecipitation kit. Equal amounts of whole cell lysates (500 μg protein) were mixed with mouse anti-Nrf2 antibody, non-immune mouse serum (negative control), or mouse anti-ubiquitin antibody (positive control), specificities of which have been reported [28]. Protein A/G agarose beads were added and incubated overnight at 4 °C. The bound proteins were eluted using 30 μL of Laemmli buffer. The samples were subjected to immunoblotting and probed for ubiquitin, using a rabbit anti-ubiquitin antibody. Reverse co-immunoprecipitation was performed using the same method; cell lysates were mixed with mouse anti-ubiquitin antibody, non-immune mouse serum (negative control), or mouse anti-Nrf2 (positive control) and the bound proteins were subjected to immunoblotting and probed for Nrf2, using a rabbit anti-Nrf2 antibody, specificity of which has been reported [28].

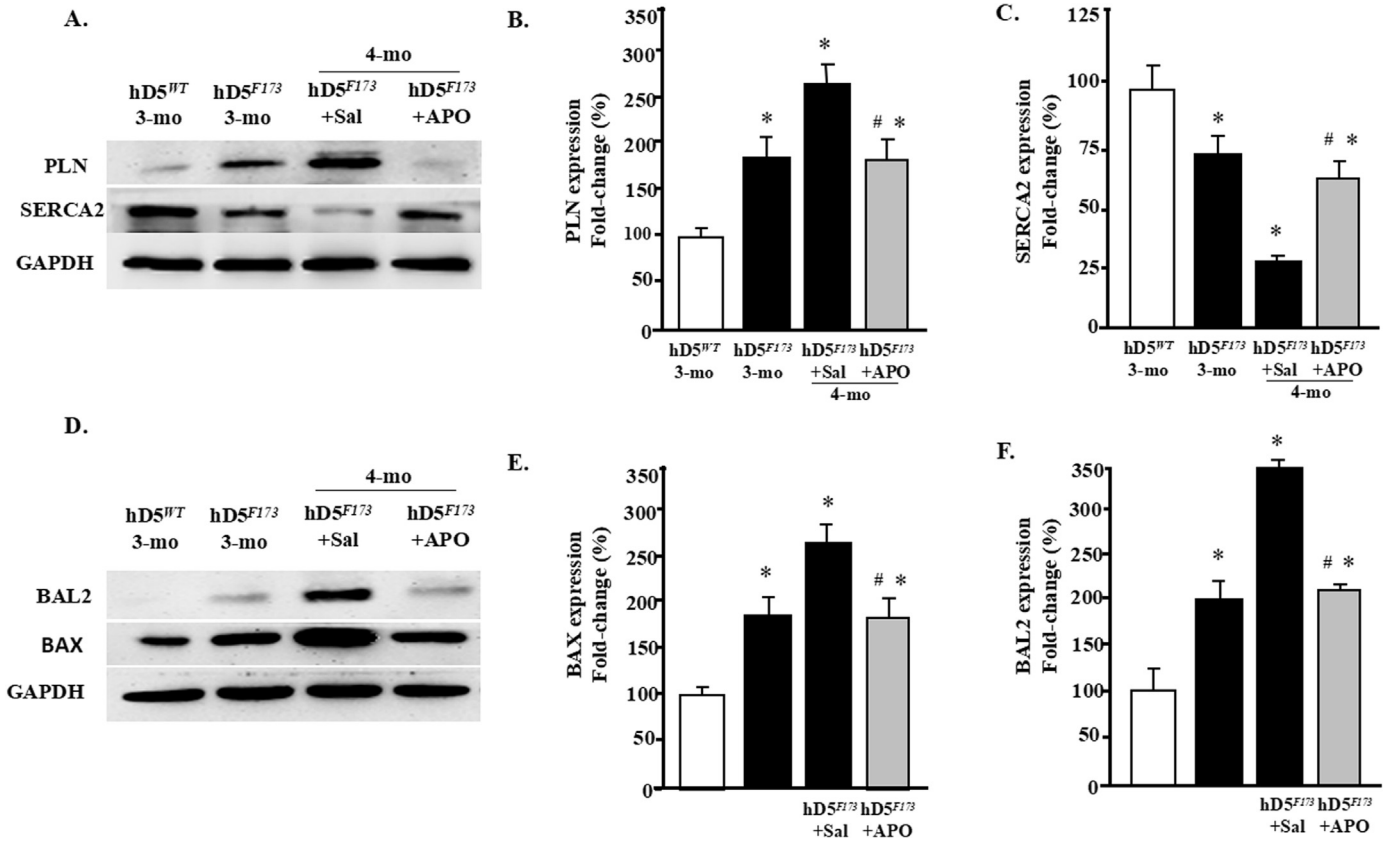

Fig. 7. D5R deficiency induces cardiomyocyte dysfunction A–C: Total proteins were extracted from hearts of 3-month-old cardiac-specific human $D5^{WT}$-TG ($hD5^{WT}$) and $hD5^{F173L}$-TG ($hD5^{F173}$) and 4-month-old cardiac-specific $hD5^{F173}$ mice treated with saline ($hD5^{F173L}$ + Sal) or apocynin ($hD5^{F173L}$ + APO) for 4 weeks, starting at 3 months of age (n = 12 mice/group). PLN and SERCA2 expression was semiquantified by western blot. **D–F:** BAL2 and BAX expression was semi-quantified by western blot. *P < 0.05 vs. $hD5^{WT}$ mice; #P < 0.05 vs. $hD5^{F173L}$ + Sal.

2.13. Statistical analysis

The data are expressed as mean ± SEM. Significant differences between and among groups were determined by one-way or two-way factorial ANOVA, Holm-Sidak test, for groups > 2 and the Student's *t*-test for groups = 2. Overall survival was analyzed with the Kaplan-Meier method and the log-rank test. P < 0.05 was considered to indicate a statistically significant difference. All statistical analyses were performed using SPSS 22.0 statistical software (SPSS, Inc., Chicago, IL, USA).

3. Results

3.1. DCM in cardiac-specific $hD5^{F173L}$-TG and $hD5^{WT}$-TG mice

We generated cardiac-specific $hD5^{F173L}$-TG and $hD5^{WT}$-TG mice expressing the mutant human D5R, $hD5^{F173L}$, and wild-type human D5R, $hD5^{WT}$, under the control of the α-MHC promoter. Three-month-old $hD5^{F173L}$-TG mice had DCM (Fig. 1**A**) with advanced heart failure (Fig. 1**A–G**), associated with increased myocardial fibrosis observed by Masson's trichrome staining (Fig. 1**B**). LV M-mode allows the assessment of LV systolic function. Systolic and diastolic LV internal volume (LVIVs and LVIVd, respectively) and systolic and diastolic LV internal diameter (LVIDs and LVIDd, respectively) were measured from the M-mode images at the level of the papillary muscles. LV ejection fraction (EF) and LV fractional shortening (FS) were used to evaluate LV global systolic function [29]. Cardiac-specific $hD5^{F173L}$-TG mice, relative to cardiac-specific $hD5^{WT}$-TG mice, had increased LVIVs (44.97 ± 14.54 vs. 24.66 ± 5.34 μL) and LVIVd (83.99 ± 18.42 vs. 64.83 ± 9.90 μL) (P < 0.01) (Fig. 1**C**) and enlarged LVIDs (3.26 ± 0.42 vs. 2.58 ± 0.23 mm) and LIVDd (4.28 ± 0.39 vs. 3.86 ± 0.25 mm) (P < 0.05) (Fig. 1**D**), as well as impaired EF (42.01 ± 8.73% vs. 53.18 ± 4.84%) (Fig. 1**E**) and FS (21.23 ± 5.15% vs. 29.95 ± 3.52%, P < 0.05) (Fig. 1**F**). The hearts/body rate were significantly higher in $hD5^{F173L}$-TG than $hD5^{WT}$-TG mice (Fig. 1**G**). These results show that cardiac-specific D5R deficiency results in DCM, indicating that the D5R may have a cardioprotective effect.

3.2. Dopamine D5 receptor deficiency facilitates NOX assembly at the plasma membrane and increases NADPH oxidase activity and ROS generation

The impaired D5R-negative regulation of NADPH oxidase activity contributes to the pathogenesis of hypertension in global $D5^{-/-}$ mice [7,11]. Cardiac NADPH oxidase activity (Fig. 2**A**) and ROS generation (Fig. 2**B**) were significantly increased in 3-month-old cardiac-specific $hD5^{F173L}$-TG, relative to cardiac-specific $hD5^{WT}$-TG mice. Notably, the reduction in D5R activity was associated with increased translocation of NADPH oxidase regulatory subunits $p40^{phox}$ and $p47^{phox}$ to the plasma membrane **(**Fig. 2**C–E).**

For the in vitro study, H9c2 cells were stably transfected with $hD5R^{F173L}$ (H9c2-$hD5^{F173L}$) or $hD5R^{WT}$ (H9c2-$hD5^{WT}$). NADPH oxidase activity, ROS production, and basal protein expressions of $p40^{phox}$ and $p47^{phox}$ were higher in H9c2-$hD5^{F173L}$ than H9c2-$hD5^{WT}$ cells (Fig. 2**F**), consistent with the in vivo study.

Apocynin has been used as an efficient NADPH oxidase inhibitor by impairing the translocation of the NADPH-oxidase complex cytosolic components, $p47^{phox}$ and $p40^{phox}$, to the plasma membrane [7,18–20], which may be a therapeutic target for the treatment of advanced heart failure [30]. Therefore, we determined if inhibition of NADPH oxidase

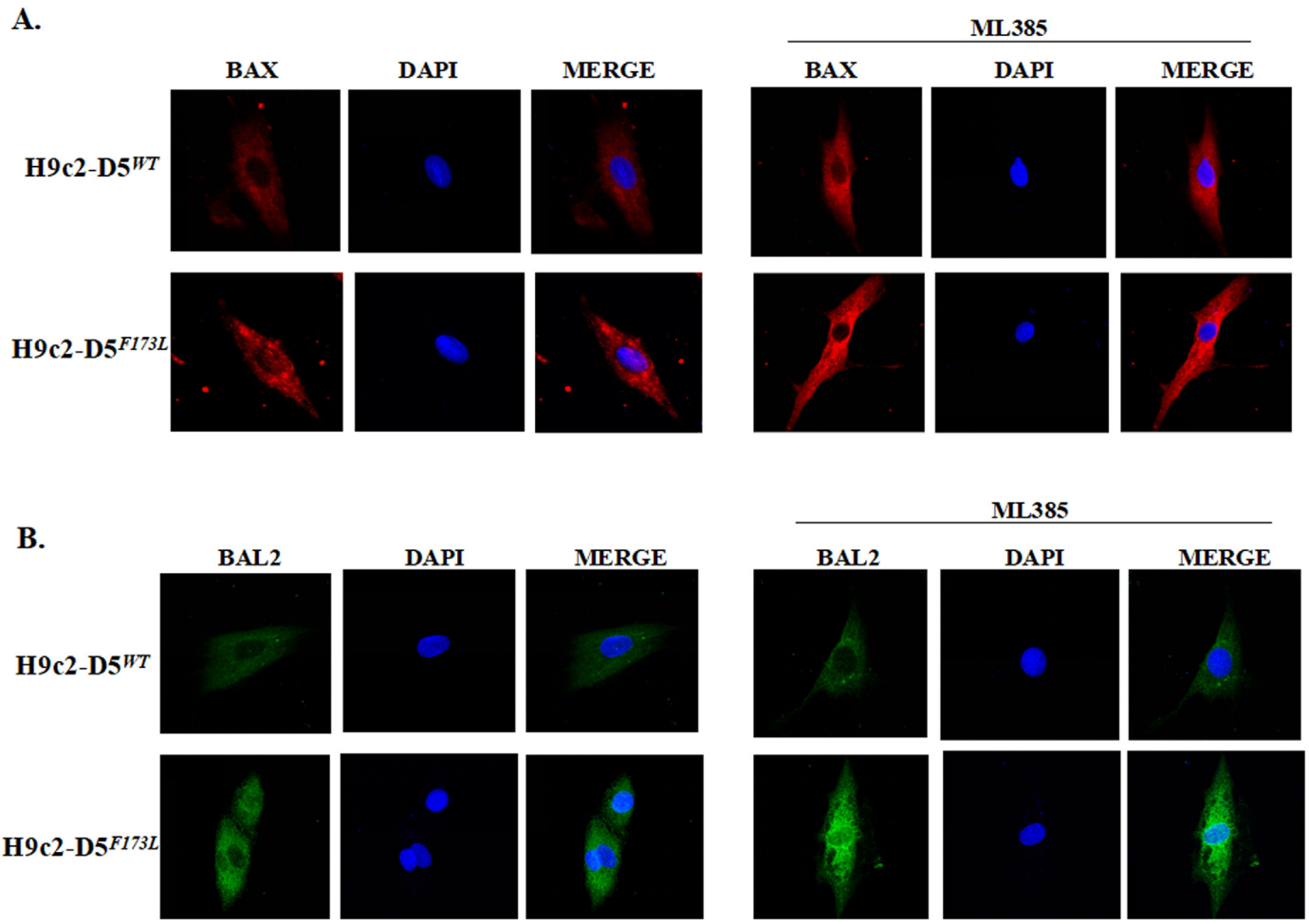

Fig. 8. D5R deficiency induces cardiomyocyte injury that is aggravated by Nrf2 inhibition. A: and **B:** H9c2-D5^{WT} and H9c2-D5^{F173L} cells were treated with ML385 (1 μM), an inhibitor of Nrf2, for 12 h. Cytosol BAX (**B**) and BAL2 (**C**) expressions are increased by ML385 treatment. **Red:** BAX; **Blue:** DAPI; and **Green:** BAL2.

activity prevents the progression of DCM in cardiac-specific hD5^{F173L}-TG mice by treatment with apocynin (1 mmol/kg/day). Cardiac-specific hD5^{F173L}-TG mice (3-month-old), treated with saline or apocynin, had similar body weights throughout the experimental period (Supplementary Tables 1 and 2). The intraperitoneal injection of apocynin that was started at 3 months of age (pretreatment) and continued for four weeks until 4 months of age decreased cardiac NADPH oxidase activity to the 3-month-old hD5^{WT}-TG level (Fig. 2**A**) and the translocation of p47^{phox} and p40^{phox} to the plasma membrane ($P < 0.05$) (Figs. 2**C–E**), compared with the saline-treated group. ROS production was decreased by apocynin treatment (Fig. 2**B**), which was associated with a reduction in NADPH oxidase activity (Fig. 2**A**).

3.3. Cardiac-specific dopamine D5 receptor mutation induces a mitochondria-independent increase in reactive oxygen species levels in heart

Within cardiomyocytes, ROS are generated in different compartments by different enzymes. In addition to the NADPH oxidases, mitochondria are one of the most important cellular source of ROS [31]. To gain insight into the source and the potential mechanism of D5R mutation-induced generation of ROS in human cells, we analyzed the mitochondrial ROS and function of this process.

ROS levels of Mitochondrial were measured by using the mitochondrial-specific probe MitoSox. Compared with significant increase in intracellular ROS levels, a little bit higher in mitochondrial superoxide was observed, which was not significant either in cardic specific D5R^{F173L}-TG mice or in H9c2-hD5^{F173L} cell ($P > 0.05$) (Fig. 3**A and B**). The role of mitochondrial function was also detected in cardic specific D5R^{WT}-TG and D5R^{F173L}-TG mice (3 months). The mRNA expression of complex I genes(Ndufs4 and Ndufb6) remained unaltered. The mRNA levels of several genes representative of the ETC complexes II–IV also remained unchanged (Fig. 3**C**). Complex activities measured in isolated mitochondrial complexes (complex I–IV) showed slight decresed in cardic specific D5R^{F173L}-TG mice compared to D5R^{WT}-TG mice (3 months) ($P > 0.05$). A parallel decrease in complexes activity was observed in H9c2-D5^{F173} cells ($P > 0.05$) (Fig. 3**D and E**). These data shows that cardic specific D5R mutantion transfection did not affect mitochondria function and mitochondrial ROS production. Although mitochondria are the crucial source of ROS response in cardiomyocytes of D5R^{F173L}-TG mice, but cardic specific D5R mutantion transfection increased ROS production may mainly come from NADPH oxidase.

3.4. Apocynin ameliorates the cardiac enlargement and heart injury in cardiac-specific D5R deficiency-induced DCM

Apocynin had a favorable effect on cardiac performance (Fig. 4**A**) but had a minimal effect on heart/body rate in cardiac-specific hD5^{F173L}-TG mice (4-month-old) (Fig. 4**B**). The administration of apocynin for 4 weeks in 3-month old hD5^{F173L}-TG mice improved all of the measures (LVIV, LVID, EF, and FS) of cardiac performance (LVIVs: 41.97 ± 10.21 vs. 52.66 ± 6.11 μL; LVIVd: 80.98 ± 9.42 vs. 89.24 ± 12.90 μL $P < 0.05$; LVIDs: 3.11 ± 0.45 vs. 3.76 ± 0.13 mm; LVIDd: 4.28 ± 0.38 vs. 4.66 ± 0.23 mm $P < 0.01$) (Fig. 4**C** and **D**). Pump failure (% EF: 40.15 ± 5.62% vs.

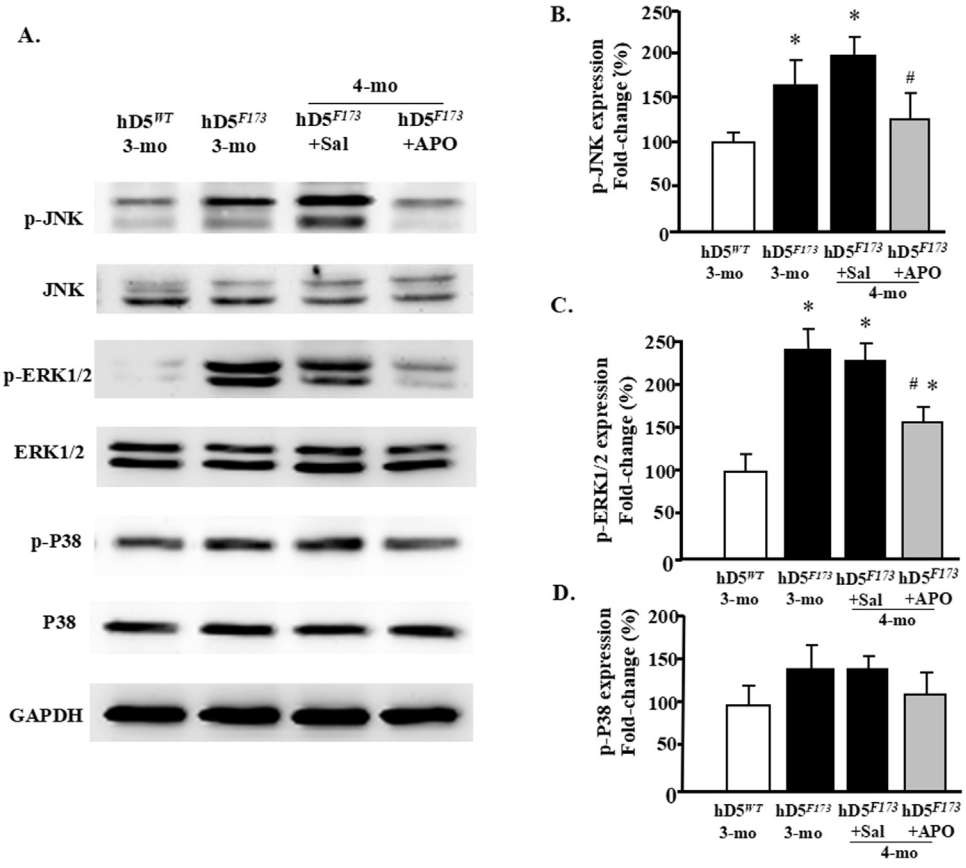

Fig. 9. D5R functional deficiency upregulates p-JNK and p-ERK1/2. Proteins were extracted from hearts of 3-month-old cardiac-specific hD5^{WT}-TG (hD5^{WT}) and hD5^{F173L}-TG (hD5^{F173}) and 4-month-old cardiac-specific hD5^{F173} mice treated with saline (hD5^{F173L} + Sal) or apocynin (hD5^{F173L} + APO) for 4 weeks, starting at 3 months of age (n = 12 mice/group). Protein expression was semi-quantified by western blot using anti-p-JNK and anti-p-ERK1/2. **A:** and **B:** p-JNK, **A:** and **C:** p-ERK1/2, (**D**) p-P38 (n = 10 mice/group). The data were normalized with total ERK1/2, total JNK, and total P38; *P < 0.05 vs. hD5^{WT} mice; #P < 0.05 vs. hD5^{F173L} + Sal.

31.23 ± 4.44%; % FS: 25.38 ± 5.04% vs. 17.05 ± 6.23%, P < 0.05) was also alleviated by apocynin (Fig. 4**E** and **F**). These results demonstrate that inhibition of NADPH oxidase significantly delays the progression of DCM caused by the cardiac-specific deficiency of D5R function. However, the apocynin-induced decrease in ROS production was not as large as the decrease in NADPH oxidase activity (Fig. 2**A** and **B**), which indicates that there is some counter-regulation of the apocynin-induced reduction in NADPH oxidase activity.

3.5. Dopamine D5 receptor deficiency impairs Nrf2 antioxidant activity

Activation of Nrf2 and its target genes plays an important role in protecting organs, including the heart, against pathological cardiac remodeling by suppressing oxidative stress [32,33]. To determine if Nrf2-induced antioxidant function is affected by D5R deficiency-induced DCM, we studied the expression (Fig. 5) and ubiquitination (Fig. 6) of Nrf2 in the nucleus and cytoplasm. Cardiac-specific D5R deficiency slightly increased nuclear Nrf2 expression at 3 months of age (+ 12 ± 4%, hD5^{F713L}-TG mice (3-month-old) vs. hD^{WT}-TG) but significantly decreased it at 4 month of age (− 28 ± 2%, hD5^{F173L}-TG + Sal (4-month-old) vs. hD^{WT}-TG) (Fig. 5**A**); apocynin did not affect Nrf2 translocation into the nucleus in hD5^{F173L}-TG + Apo at 4 months of age. The nuclear expression of NAD(P)H quinone 1 dehydrogenase (NQO1), which, prevents the reduction in one electron of quinones and heme oxygenase 1 (HO1), which removes toxic heme and produces antioxidants, such as biliverdin carbon monoxide [33]. NQO1 and HO-1, downstream targets of Nrf2 [29,33], also increased at 3 months of age and decreased toward the 3 month old level at 4 months of age (hD5^{F713L}-TG (3-month-old) vs. hD5^{F173L}-TG + Sal (4-month-old)). Similar to the Nrf2 results (Fig. 5**A**), apocynin had no effect of NQO1 and HO1 expression in 4-month-old hD5^{F173L}-TG mice (D5^{F173L}-TG + Sal vs. hD5^{F173L}-TG + Apo) (Figs. 5**B** and **C**). ROS stimulate the translocation of Nrf2 from the cytoplasm into the nucleus [34]. Therefore, it is possible that the increased nuclear Nrf2 expression at 3 months of age is a compensation for the increase in ROS production in hD5^{F173L}-TG mice. Immunofluorescence microscopy of H9C2 cells showed that Nrf2 was located mainly in the cytoplasm of H9c2-hD5^{WT} cells, while nuclear expression of Nrf2 was increased in the nucleus in H9c2-hD5^{F173L}cells (cyan color, Fig. 5**D**). Immunoblotting also showed that nuclear, but not total Nrf2, as well as cytoplasmic NQO1 and HO1 expressions were significantly increased in H9c2-hD5^{F173L} compared with H9c2-hD5^{WT}cells, which were consistent with the in vivo study in 3-month-old but not 4-month-old mice (Fig. 5**E**). However, total Nrf2 expression was not different between two cells, which further confirmed the hypothesis that cardiac-specific functional deficiency of D5R affects the translocation of Nrf2 in nucleus but not its total expression.

3.6. Dopamine D5 receptor deficiency increases Nrf2 degradation via the ubiquitin-proteasome pathway

Nrf2 degradation is regulated by Nrf2 ubiquitination [28,34]. Therefore, we determined if cardiac D5R could increase the stability of Nrf2 protein, by reducing its ubiquitination via the proteosome pathway. We immunoprecipitated Nrf2 from heart homogenates of hD5^{WT}-TG and hD5^{F173L}-TG mice at 3- and 4 months of age and immunoblotted the immunoprecipitates with anti-ubiquitin antibody. We corroborated the results by reversing the order of immunoprecipitation and immunoblotting, i.e., immunoprecipitation with ubiquitin and immunoblotting with Nrf2 antibody (Fig. 6**A** and **B**) The amount of ubiquitinated Nrf2 was slightly, but not significantly, decreased in hD5^{F173L}-TG mice at 3 months of age but was significantly increased in hD5^{F173L}-TG mice at 4 months of age, suggesting that the decrease in the nuclear Nrf2 expression in hD5^{F173L}-TG mice at 4 months of age may be the result of increased Nrf2 degradation of ubiquitinated Nrf2 in the nucleus.

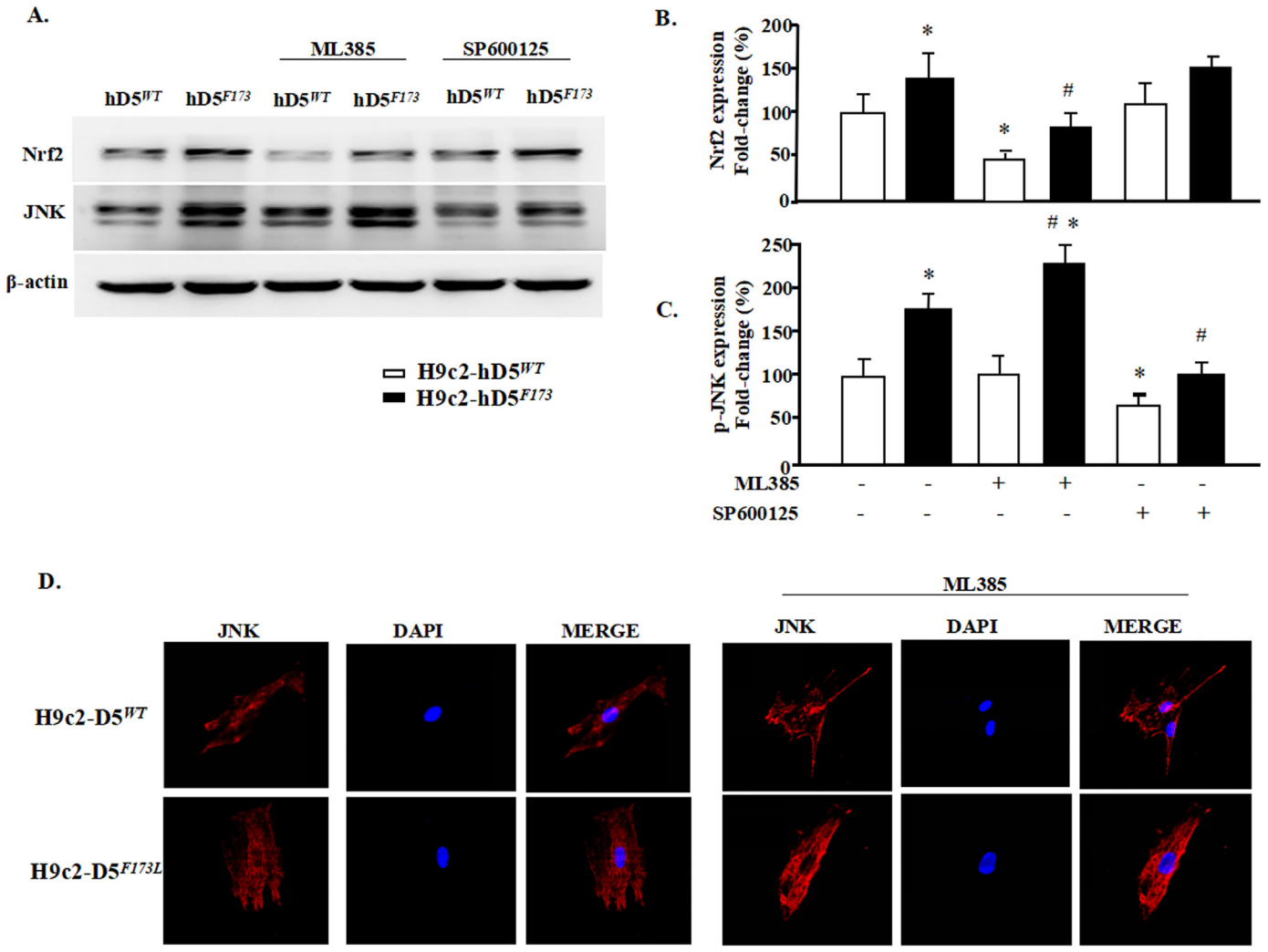

Fig. 10. JNK pathway is downstream of Nrf2. H9c2-D5^{WT} and H9c2-D5^{F173L} cells were treated with ML385 (1 μM), an inhibitor of Nrf2, or SP600125 (10 μM), an inhibitor of JNK, for 12 h. JNK inhibition does not affect Nrf2 expression (**A** and **C**). However, Nrf2 inhibition (**A, B, D**) increases further the D5R functional deficiency-induced increase in JNK in H9c2-D5^{F173L} cells. *P < 0.05 vs. untreated H9c2-D5^{WT} cells. #P < 0.05 vs. untreated H9c2-D5^{F173L} cells. n = 8/group.

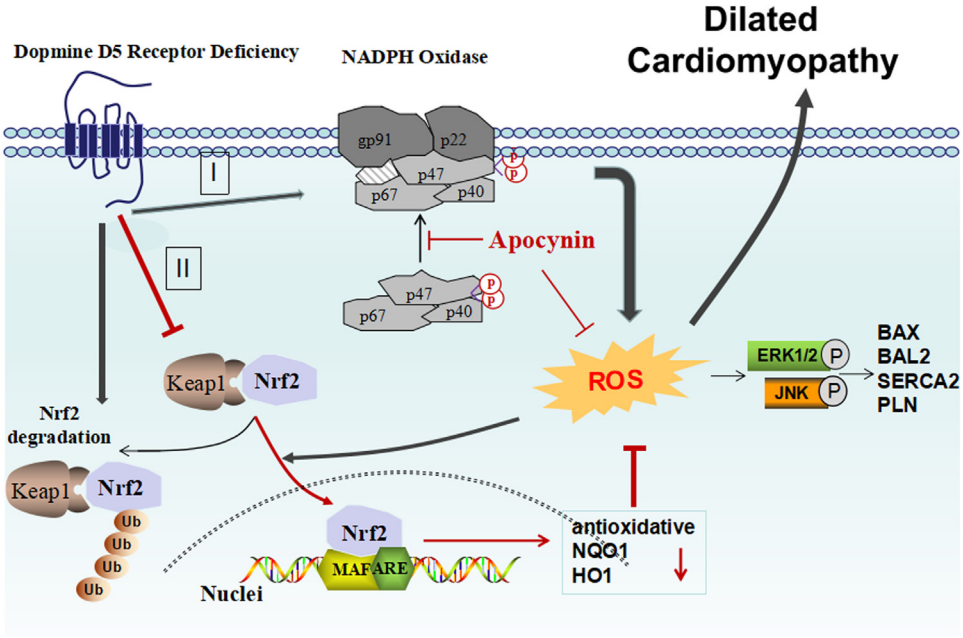

Fig. 11. D5R mutation induces dilated cardiomyopathy that is related to oxidative stress. D5R deficiency causes an increase in NADPH oxidase activity (I), and prevents the translocation of Nrf2 into the nucleus (II), resulting in a failure of the transcription of a number of antioxidative genes via masculoaponeurotic fibrosarcoma (MAF) and antioxidant response elements (ARE). Antioxidant proteins include NAD(P)H quinone 1 dehydrogenase (NQO1) and heme oxygenase 1 (HO1). Oxidative stress accelerates the signaling of the ERK1/2 and JNK pathway, impairing the balance between apoptosis (BCL2 associated X, apoptosis regulator [*BAX*]) and anti-apoptosis (B aggressive lymphoma protein 2 (BAL2, *PARP14* gene). Phospholamban (PLN) is also stimulated which inhibits cardiac muscle sarcoplasmic/endoplasmic reticulum Ca^{2+}-ATPase (SERCA, encoded by *ATP2A2*), which in turn causes cardiac remodeling and finally, dilated cardiomyopathy. D5R deficiency also allows Kelch-like ECH Associated Protein 1 (Keap1) to target Nrf2 in the cytoplasm for ubiquitination and degradation in the proteasome.

3.7. Dopamine D5 receptor deficiency induces cardiomyocyte dysfunction

Disrupted cardiomyocyte Ca^{2+} homeostasis is recognized as a major contributor to the systolic and diastolic dysfunction phenotype. In our study, the expression of cardiac phospholamban (PLN), which regulates cardiac sarcoplasmic reticulum Ca^{2+} ATPase (SERCA), was increased in cardiac-specific $hD5^{F173L}$-TG mice at 3 months of age and increased further at 4 months of age ($hD5^{F173L}$-TG + Sal) (Fig. 7**A**). PLN was decreased by apocynin treatment in 4-month-old mice to the 3-month old $hD5^{F173L}$-TG level (Fig. 7**A**). By contrast, SERCA expression was decreased in cardiac-specific $hD5^{F173L}$-TG mice at 3 months of age and was even more decreased at 4 months of age ($hD5^{F173L}$-TG + Sal mice). Apocynin increased SERCA expression in the 4-month-old $hD5^{F173L}$-TG level to the 3-month-old $hD5^{F173L}$-TG level (Fig. 7**C**). We also measured the expression of apoptosis and myocardial injury markers BAX (BCL2 associated X, apoptosis regulator) and BAL2 (B aggressive lymphoma protein 2) and found that their expressions were increased in $hD5^{F173L}$-TG mice at 3 months of age and increased further at 4 months of age in $hD5^{F173L}$-TG ($hD5^{F173L}$-TG + Sal mice) (Fig. 7**E** and **F**). As with the PLN results, apocynin treatment decreased the BAX and BAL2 in the 4-month-old $hD5^{F173L}$-TG + Apo mice to the same level as that found in 3-month-old $D5^{F173L}$-TG mice (Fig. 7**D–F**). These results indicate that D5R deficiency-induced ROS overproduction accelerates cardiomyocyte disruption of Ca^{2+} homeostasis and promotes apoptosis, in vivo. In vitro studies also showed that H9c2-$hD5^{F173L}$ cells have increased BAL2 and BAX expression compared with H9c2-$hD5^{WT}$cells **(**Supplementary Fig. 2**)**. Treatment with the Nrf2 inhibitor ML385, which decreased Nrf2 expression in the cytoplasm and nucleus (Supplementary Fig. 3), increased further the already increased expression of BAX and BAL2 in H9c2-$hD5^{F173L}$, relative to H9c2-$hD5^{WT}$cells (Fig. 8**A** and **B**), which would aggravate the cardiomyocyte apoptosis. These data confirm that Nrf2 plays an important role in the D5R deficiency-induced cardiomyocyte dysfunction.

3.8. JNK/ERK pathway is activated by ROS in D5R deficiency-induced DCM

ROS induction of the MAPK signaling pathway may take part in the progression of DCM [35]. Therefore, we next determined if ERK, JNK, or p38 is involved in the D5R functional deficiency-induced DCM in $hD5^{F173L}$-TG mice. We found that basal cardiac phospho-JNK (p-JNK) and phospho-ERK1/2 (p-ERK1/2) protein expressions but not their total protein expressions were higher in $hD5^{F173L}$-TG than $hD5^{WT}$-TG mice both at 3 months ($hD5^{F173}$) and 4 months ($hD5^{F173}$ + Sal) of age (Fig. 9**A–C**). By contrast, phospho- or total-P38 was not affected by the $hD5^{F173}$ mutation (Fig. 9**A**and **D**). ROS increased the phosphorylation and presumably the activity of these proteins because the increased p-JNK and p-ERK1/2 protein expressions in both ($hD5^{F173L}$) 3-month- and ($hD5^{F173}$ + Sal) 4-month-old mice were decreased by apocynin treatment in (Fig. 9**A–C**). These results indicate that ROS participate in the activation of JNK and ERK pathways in D5R functional deficiency-induced DCM.

To determine further whether ERK and JNK are downstream effects of Nrf2 and ROS, we treated H9c2-$hD5^{F173L}$ cells with Nrf2 (ML385) [16] and JNK (SP600125) [17] inhibitors. The Nrf2 inhibitor, as expected, decreased Nrf2 expression in H9c2-$D5^{WT}$ cells and also decreased the slight increase in Nrf2 expression in H9c2-$hD5^{F173L}$ cells but not to the same level as that found in H9c2-$D5^{WT}$ cells (Fig. 10**A** and **B**). The Nrf2 inhibitor had no effect on p-JNK expression in H9c2-$D5^{WT}$ cells but increased the expression of total JNK in H9c2-$hD5^{F173L}$ cells. (Fig. 10**A** and **C)**. By contrast, inhibition of JNK was unable to alter total Nrf2 expression (Fig. 10**B** and **C**) in either H9c2-$D5^{WT}$ or H9c2-$hD5^{F173L}$ cells. These results demonstrated that increased ROS production stimulates the ERK/JNK pathway, in part via a decrease in Nrf2 expression, which participates in the D5R functional deficiency-induced DCM.

4. Discussion

Cardiovascular diseases are closely linked to hypertension. The risk of DCM, characterized by ventricular dilatation and impaired systolic and diastolic function, is doubled when the blood pressure exceeds 160/95 mmHg [36]. A recent estimate indicated that the risk for cardiovascular disease for each 10 mm Hg increment in systolic blood pressure from baseline is 25% for women and 15% for men in the USA [37]. Genome-wide linkage studies have revealed that the loci of the human D5R (hD5R), 4p15.1–16.1, and its pseudo genes, 1q21.1 2p11.1-p11.2, are linked to essential hypertension [9,38,39]. Moreover, $hD5^{F173L}$ has diminished cAMP activity and D5R function, which transgenosis in mice signifiantly inhibit endogenous D5R expression (Supplementary Fig. 1). We have found that global $hD5^{F173L}$-TG mice have high blood pressure and cardiac hypertrophy [10]. In our current study, the blood pressures of cardiac-specific $hD5^{F173L}$-TG mice were normal and not significantly different from those observed in cardiac-specific $hD5^{WT}$-TG mice at 3 months of age (Supplementary Fig. 4A) and 4 months of age (not shown). Therefore, the DCM in cardiac-specific $hD5F^{173L}$-TG mice is a direct cardiac effect of the mutant human D5R gene rather than a compensatory dilatation due to pressure overload. We now highlight the observation that D5R is necessary for the normal expression of Nrf2 and inhibition of NADPH oxidase activity and that their dysfunctions stimulate ROS over-production and myocardial remodeling via ERK1/2/JNK pathway (Fig. 11**).**

Oxidative stress has been identified as one of the key contributing factors in the pathogenesis of heart disease, including myocardial hypertrophy, myocardial remodeling, DCM, and heart failure [30,40–42]. We have reported that global $D5^{-/-}$ mice have increased ROS production, associated with increased expression and activity of NADPH oxidase and phospholipase D in the kidney [7,10,11]. We have also reported that renal and brain NADPH oxidase activity is increased in global $hD5^{F173L}$-TG mice [7,10,11]. NADPH oxidases are the major sources of ROS in many cells, including cardiac, vascular endothelial, and renal epithelial cells [7,10,11,17–19,30,41–45]. NADPH oxidases, depending on the particular isoform, are multi-subunit enzymatic complexes consisting of membrane subunits gp91phox and p22phox and cytosolic subunits p47phox, p67phox, and p40phox [40–44]. In our current study, we found that membrane p40phox and p47phox levels were markedly increased in the heart of cardiac-specific $hD5^{F173L}$-TG mice that had DCM. Apocynin decreases ROS production and inhibits NADPH oxidase activity by blocking the translocation of cytosolic subunits p47phox and p40phox to the plasma membrane [7,17–19]. However, the apocynin-mediated reduction of cardiac ROS production was smaller than the reduction of NADPH oxidase activity which could be taken to indicate that factors other than oxidative stress are important in the pathogenesis of DCM in cardiac-specific $hD5^{F173L}$-TG mice.

In addition to the NADPH oxidases, mitochondria are one of the most important cellular source of ROS in cardiomyocytes [31]. Human studies on heart failure as well as animal models on cardiovascular diseases suggest that mitochondrial bioenergetics deficiency may contribute to the development and progression of the disease [46,47]. we found that mitochondria function and mitochondrial ROS was similar in $D5R^{F173L}$-TG mice and $D5R^{WT}$-TG mice. H9c2-$hD5^{F173L}$ cells also have normal mitochondria function, which was similar with H9c2-$hD5^{WT}$ cells. These data indicate that cardic specific D5R mutantion transfection increased ROS production may mainly come from NADPH oxidase but not from mitochondria, and the role of NADPH oxidase in the regulation of DCM may extend beyond ROS, which is unlikely. A better possibility is that ROS can stimulate the activity of antioxidant proteins that could serve as a negative feedback, Nrf2 for example [32,33].

Several clinical studies have shown that the antioxidant effect of Nrf2 is a critical regulator for maintaining the structural and functional integrity of the heart in states of oxidative stress [32,33]. We have reported that the dopamine D2 receptor is necessary for normal Nrf2

activity in the kidney [28]. Renal-selective silencing of *Drd2* in the mouse increases ROS production which is partly mediated by increased Nrf2 degradation [28]. The D5R also inhibits ROS production, not only by inhibiting NADPH oxidase activity, but also by increasing HO-1 expression and activity [7,11,48]. In our current study, cardiac-specific hD5^{F173L}-TG mice had increased Nrf2 expression at 3 months of age but decreased Nrf2 expression at 4 months of age because of increased ubiquitination and subsequent degradation. We suggest that the increased cardiac Nrf2 expression at 3 months of age may be a mechanism to counteract the state of oxidative stress but eventually fails. This could also explain why Nrf2 expression was increased in H9c2-hD5^{F173L} cells and its inhibition increased p-JNK expressions, a marker of tissue injury. The finding that D5R deficiency prevents the nuclear translocation of Nrf2, impairing the upregulation of the expression of antioxidant enzymes, e.g., HO1, highlights the important role of cardiac ROS and oxidative stress in myocardial dysfunction.

Increased generation of ROS in cardiomyocytes leads to increased necrosis and apoptosis, which induce cardiac remodeling and dysfunction [49]. Oxidative stress accelerates inflammation and apoptosis, which in turn cause cardiomyocyte hypertrophy and fibroblast proliferation, resulting in the cardiac remodeling [50]. In our current report, echocardiographic studies showed that the decrease in ROS production caused by apocynin was associated with a decrease in cardiac dilatation and an improvement in cardiac function; heart weight was also decreased. The apocynin-mediated beneficial effects in the myocardium, including the reduction in DCM, was associated with a decrease in apoptosis (BAX) and anti-apoptosis (BAL2) proteins, a decrease in PLN, but an increase in SERCA2 in hD5^{F173L}-TG mice. H9c2-hD5^{F173L} cells showed that the Nrf2 inhibitor [15] increased the expression of p-JNK, which plays a key role in tissue injury [51]. Our data indicate that Nrf2 and NADPH oxidase regulate ROS production involved in the promotion of hD5^{F173L}-mediated cardiac dysfunction and DCM. DCM is a common cause of heart failure due to the progressive depression of myocardial contractile function and ventricular dilatation [1–5]. We found that more than 60% of the cardiac-specific hD5^{F173L}-TG mice did not survive after 6 months of age (Supplementary data 4B). The etiology of the early death of cardiac-specific hD5^{F173L}-TG mice may be due to heart failure.

In the dilated failing heart, multiple signaling pathways are activated, including ERK1/2, JNK,P38a MAP kinases, and AKT [52]. There is increasing evidence that NADPH oxidase plays an important role in modulating ERK1/2 and AKT activity in the myocardium undergoing ischemia-reperfusion injury [35]. In this study, we found that the levels of p-ERK1/2 and p-JNK but not p-P38 were increased in the heart of cardiac-specific hD5^{F173L}-TG mice. The increased expression of p40 and p47 was also accompanied by increased levels of p-ERK1/2 and p-JNK in H9c2-D5^{F173L}-cells compared with H9c2-D5^{WT} cells. The levels of p-ERK1/2 and p-JNK in the hearts of cardiac-specific hD5^{F173L}-TG mice, which were increased than in hD5^{F173L}-TG mice, were decreased by apocynin. The in vitro studies also demonstrated that ERK1/2 and JNK are the downstream of Nrf2 pathway. Therefore, p-ERK1/2 and p-JNK are involved in the D5R deficiency-induced DCM, which are up-regulated by NADPH oxidase and Nrf2-deficiency-stimulated ROS production.

Ca^{2+} plays a pivotal role in the normal cardiac function and pathogenesis of cardiac disease [53,54]. Ca^{2+}-handling abnormalities have been found in various forms of heart failure, including DCM [55–57]. Indeed, in our cardiac-specific hD5^{F173L} TG mice, SERCA2 expression was decreased, relative to cardiac-specific hD5^{WT} TG mice, indicating an abnormal transduction of SERCA2 with D5R dysfunction. By contrast, the levels of PLN, a negative regulator of SERCA [58], were increased in cardiac-specific hD5^{F173L} TG mice, especially at 4 months of age, indicating that a dysfunction of SERCA2 may take part in the progression of D5R deficiency-induced DCM. Therefore, the D5R negatively regulates NADPH oxidase activity, probably by adjusting the concentration of intracellular Ca^{2+} ion. However, the detailed mechanism of the D5R-mediated regulation of SERCA2 remains to be clarified.

5. Conclusion

In summary, our result shows that the cardiac D5R is necessary for maintaining normal heart function. We demonstrated that the cardiac-specific decrease in D5R function, caused by the cardiac-specific expression of hD5^{F173L}, results in DCM accompanied by increased ROS production come from cardiac NADPH oxidase and Nrf2 degradation but not mitochondria and stimulation of ERK1/2/JNK activities, accompanied by an increase in pro-apoptotic BAX and anti-apoptotic BAL2, an increase in PLN, and a decrease in SERCA2. Modulation of cardiac D5R could be a therapeutic approach in DCM.

Funding sources

These studies were supported, in part, by grants from Chinese Academy of Medical Sciences Innovation Fund for Medical Sciences (CIFMS, 2016-I2M-1-016), National Natural Science Foundation (China) (81600334, 81670387), Life science society consortium "Youth Talent Promotion Project"and National Institutes of Health (USA) (P01HL074940, PAJ).

Appendix A. Supplementary material

Supplementary data associated with this article can be found in the online version at doi:10.1016/j.redox.2018.07.008.

References

[1] S.E. Hughes, W.J. McKenna, New insights into the pathology of inherited cardiomyopathy, Heart 91 (2005) 257–264.
[2] D. Fatkin, R.M. Graham, Molecular mechanisms of inherited cardiomyopathies, Physiol. Rev. 82 (2002) 945–980.
[3] J.G. Seidman, C. Seidman, The genetic basis for cardiomyopathy: from mutation identification to mechanistic paradigms, Cell 104 (2001) 557–567.
[4] J.L. Jefferies, J.A. Towbin, Dilated cardiomyopathy, Lancet 375 (2010) 752–762.
[5] S.R. Houser, K.B. Margulies, A.M. Murphy, F.G. Spinale, G.S. Francis, S.D. Prabhu, H.A. Rockman, D.A. Kass, J.D. Molkentin, M.A. Sussman, W.J. KochAmerican Heart Association Council on Basic Cardiovascular Sciences, Council on Clinical Cardiology, and Council on Functional Genomics and Translational Biology, Animal models of heart failure: a scientific statement from the American Heart Association, Circ. Res. 111 (2012) 131–150.
[6] R. Arsanjani, D.S. Berman, H. Gransar, V.Y. Cheng, A. Dunning, F.Y. Lin, S. Achenbach, M. Al-Mallah, M.J. Budoff, T.Q. Arsanjani, H.J. Chang, F. Cademartiri, K.M. Chinnaiyan, B.J. Chow, A. DeLago, M. Hadamitzky, J. Hausleiter, P. Kaufmann, T.M. LaBounty, J. Leipsic, G. Raff, L.J. Shaw, T.C. Villines, R.C. Cury, G. Feuchtner, Y.J. Kim, J.K. Min, C. Investigators, Left ventricular function and volume with coronary CT angiography improves risk stratification and identification of patients at risk for incident mortality: results from 7758 patients in the prospective multinational confirm observational cohort study, Radiology 273 (2014) 70–77.
[7] Z. Yang, L.D. Asico, P. Yu, Z. Wang, J.E. Jones, C.S. Escano, X. Wang, M.T. Quinn, D.R. Sibley, G.G. Romero, R.A. Felder, P.A. Jose, D5 dopamine receptor regulation of reactive oxygen species production, NADPH oxidase, and blood pressure, Am. J. Physiol. Regul. Integr. Comp. Physiol. 290 (2006) R96–R104.
[8] T.R. Hollon, M.J. Bek, J.E. Lachowicz, M.A. Ariano, E. Mezey, R. Ramachandran, S.R. Wersinger, P. Soares-da-Silva, Z.F. Liu, A. Grinberg, J. Drago, W.S. Young 3rd, H. Westphal, P.A. Jose, D.R. Sibley, Mice lacking D5 dopamine receptors have increased sympathetic tone and are hypertensive, J. Neurosci. 22 (2002) 10801–10810.
[9] A. Cravchik, P.V. Gejman, Functional analysis of the human D5 dopamine receptor missense and nonsense variants: differences in dopamine binding affinities, Pharmacogenetics 9 (1999) 199–206.
[10] X. Liu, W. Wang, W. Chen, X. Jiang, Y. Zhang, Z. Wang, J. Yang, J.E. Jones, P.A. Jose, Z. Yang, Regulation of blood pressure, oxidative stress and AT1R by high salt diet in mutant human dopamine D5 receptor transgenic mice, Hypertens. Res. 38 (2015) 394–399.
[11] Q. Lu, Y. Yang, V.A. Villar, L. Asico, J.E. Jones, P. Yu, H. Li, E.J. Weinman, G.M. Eisner, P.A. Jose, D5 dopamine receptor decreases NADPH oxidase, reactive oxygen species and blood pressure via heme oxygenase-1, Hypertens. Res. 36 (2013) 684–690.
[12] S. Cuevas, V.A. Villar, P.A. Jose, I. Armando, Renal dopamine receptors, oxidative stress, and hypertension, Int. J. Mol. Sci. 27 (2013) 17553–17572.
[13] A.A. Banday, M.F. Lokhandwala, Transcription factor Nrf2 protects renal dopamine

D1 receptor function during oxidative stress, Hypertension 62 (2013) 512–517.
[14] K.G. Cheung, L.K. Cole, B. Xiang, K. Chen, X. Ma, Y. Myal, G.M. Hatch, Q. Tong, V.W. Dolinsky, sirtuin-3 (SIRT3) protein attenuates doxorubicin-induced oxidative stress and improves mitochondrial respiration in H9c2 cardiomyocytes, J. Biol. Chem. 290 (2015) 10981–10993.
[15] A. Singh, S. Venkannagari, K.H. Oh, Y.Q. Zhang, J.M. Rohde, L. Liu, S. Nimmagadda, K. Sudini, K.R. Brimacombe, S. Gajghate, J. Ma, A. Wang, X. Xu, S.A. Shahane, M. Xia, J. Woo, G.A. Mensah, Z. Wang, M. Ferrer, E. Gabrielson, Z. Li, F. Rastinejad, M. Shen, M.B. Boxer, S. Biswal, Small molecule inhibitor of NRF2 selectively intervenes therapeutic resistance in KEAP1-deficient NSCLC tumors, ACS Chem. Biol. 11 (2016) 3214–3225.
[16] Q. Li, Y. Xiang, Y. Chen, Y. Tang, Y. Zhang, Ginsenoside Rg1 protects cardiomyocytes against hypoxia/reoxygenation injury via activation of Nrf2/HO-1 signaling and inhibition of JNK, Cell. Physiol. Biochem. 44 (2017) 21–37.
[17] M. Mora-Pale, M. Weiwer, J. Yu, R.J. Linhardt, J.S. Dordick, Inhibition of human vascular NADPH oxidase by apocynin derived oligophenols, Bioorg. Med. Chem. 17 (2009) 5146–5152.
[18] D.K. Johnson, K.J. Schillinger, D.M. Kwait, C.V. Hughes, E.J. McNamara, F. Ishmael, R.W. O'Donnell, M.M. Chang, M.G. Hogg, J.S. Dordick, L. Santhanam, L.M. Ziegler, J.A. Holland, Inhibition of NADPH oxidase activation in endothelial cells by ortho-methoxy-substituted catechols, Endothelium 9 (2002) 191–203.
[19] S. Vallejo, T. Romacho, J. Angulo, L.A. Villalobos, E. Cercas, A. Leivas, E. Bermejo, R. Carraro, C.F. Sanchez-Ferrer, C. Peiro, Visfatin impairs endothelium-dependent relaxation in rat and human mesenteric microvessels through nicotinamide phosphoribosyltransferase activity, PLoS One 6 (2011) e27299.
[20] Georgios Karamanlidis, Chi Fung Lee, Lorena Garcia-Menendez, Stephen C. Kolwicz Jr, Wichit Suthammarak, Guohua Gong, Margaret M. Sedensky, Philip G. Morgan, Wang Wang, Rong Tian, Mitochondrial complex I deficiency increases protein acetylation and accelerates heart failure, Cell Metab. 18 (2013) 239–250.
[21] E.A. Boehm, B.E. Jones, G.K. Radda, R.L. Veech, K. Clarke, Increased uncoupling proteins and decreased efficiency in palmitate-perfused hyperthyroid rat heart, Am. J. Physiol. Heart Circ. Physiol. 280 (2001) H977–H983.
[22] Yan Zhuang, Yi Li, Xuefeng Li, Qing Xie, Min Wu, Atg7 knockdown augments concanavalin A-induced acute hepatitis through an ROS-mediated p38/MAPK pathway, PLoS One 11 (2016) e0149754.
[23] J. Li, Y. Wu, X. Tian, J. Wang, M. Dong, A. Wang, S. Ma, Protective effect of HTK solution on postoperative pulmonary function in infants with CHD and PAH, Biosci. Rep. 37 (2017) 11–16.
[24] N. Engberding, S. Spiekermann, A. Schaefer, A. Heineke, A. Wiencke, M. Muller, M. Fuchs, D. Hilfiker-Kleiner, B. Hornig, H. Drexler, U. Landmesser, Allopurinol attenuates left ventricular remodeling and dysfunction after experimental myocardial infarction: a new action for an old drug? Circulation 110 (2004) 2175–2179.
[25] A. Funayama, T. Shishido, S. Netsu, T. Narumi, S. Kadowaki, H. Takahashi, T. Miyamoto, T. Watanabe, C.H. Woo, J. Abe, K. Kuwahara, K. Nakao, Y. Takeishi, I. Kubota, Cardiac nuclear high mobility group box 1 prevents the development of cardiac hypertrophy and heart failure, Cardiovasc. Res. 99 (2013) 657–664.
[26] T. Shishido, N. Nozaki, S. Yamaguchi, Y. Shibata, J. Nitobe, T. Miyamoto, H. Takahashi, T. Arimoto, K. Maeda, M. Yamakawa, O. Takeuchi, S. Akira, Y. Takeishi, I. Kubota, Toll-like receptor-2 modulates ventricular remodeling after myocardial infarction, Circulation 108 (2003) 2905–2910.
[27] K.J. Livak, T.D. Schmittgen, Analysis of relative gene expression data using real-time quantitative PCR and the ΔΔ CT method, Methods 25 (2001) 402–408.
[28] S. Cuevas, Y. Yang, P. Konkalmatt, L.D. Asico, J. Feranil, J. Jones, V.A. Villar, I. Armando, P.A. Jose, Role of nuclear factor erythroid 2-related factor 2 in the oxidative stress-dependent hypertension associated with the depletion of DJ-1, Hypertension 65 (2015) 1251–1257.
[29] Y. Tsujita, T. Kato, M.A. Sussman, Evaluation of left ventricular function in cardiomyopathic mice by tissue Doppler and color M-mode Doppler echocardiography, Echocardiography 22 (2005) 245–253.
[30] N. Parajuli, V.B. Patel, W. Wang, R. Basu, G.Y. Oudit, Loss of NOX2 (gp91phox) prevents oxidative stress and progression to advanced heart failure, Clin. Sci. 127 (2014) 331–340.
[31] K. Boengler, M. Kosiol, M. Mayr, R. Schulz, S. Rohrbach, Mitochondria and ageing: role in heart, skeletal muscle and adipose tissue, J. Cachexia Sarcopenia Muscle 8 (3) (2017) 349–369.
[32] Z. Lu, X. Xu, X. Hu, G. Zhu, P. Zhang, E.D. van Deel, J.P. French, J.T. Fassett, T.D. Oury, R.J. Bache, Y. Chen, Extracellular superoxide dismutase deficiency exacerbates pressure overload-induced left ventricular hypertrophy and dysfunction, Hypertension 51 (2008) 19–25.
[33] Y. Xing, T. Niu, W. Wang, J. Li, S. Li, J.S. Janicki, S. Ruiz, C.J. Meyer, X.L. Wang, D. Tang, Y. Zhao, T. Cui, Triterpenoid dihydro-CDDO-trifluoroethyl amide protects against maladaptive cardiac remodeling and dysfunction in mice: a critical role of Nrf2, PLoS One 7 (2012) e44899.
[34] D. Stewart, E. Killeen, R. Naquin, S. Alam, J. Alam, Degradation of transcription factor Nrf2 via the ubiquitin-proteasome pathway and stabilization by cadmium, J. Biol. Chem. 278 (2003) 2396–2402.
[35] J.X. Chen, H. Zeng, Q.H. Tuo, H. Yu, B. Meyrick, J.L. Aschner, NADPH oxidase modulates myocardial Akt, ERK1/2 activation, and angiogenesis after hypoxia-reoxygenation, Am. J. Physiol. Heart Circ. Physiol. 292 (2007) H1664–H1674.
[36] S. Yusuf, B. Pitt, A lifetime of prevention: the case of heart failure, Circulation 106 (2002) 2997–2998.
[37] Y.C. Wei, N.I. George, C.W. Chang, K.A. Hicks, Assessing sex differences in the risk of cardiovascular disease and mortality per increment in systolic blood pressure: a systematic review and meta-analysis of follow-up studies in the United States, PLoS One 12 (2017) e0170218.
[38] H. Allayee, T.W. de Bruin, K. Michelle Dominguez, L.S. Cheng, E. Ipp, R.M. Cantor, K.L. Krass, E.T. Keulen, B.E. Aouizerat, A.J. Lusis, J.I. Rotter, Genome scan for blood pressure in Dutch dyslipidemic families reveals linkage to a locus on chromosome 4p, Hypertension 38 (2001) 773–778.
[39] T. Rice, T. Rankinen, M.A. Province, Y.C. Chagnon, L. Perusse, I.B. Borecki, C. Bouchard, D.C. Rao, Genome-wide linkage analysis of systolic and diastolic blood pressure: the Quebec Family Study, Circulation 102 (2000) 1956–1963.
[40] A. Gorlach, R.P. Brandes, K. Nguyen, M. Amidi, F. Dehghani, R. Busse, A gp91phox containing NADPH oxidase selectively expressed in endothelial cells is a major source of oxygen radical generation in the arterial wall, Circ. Res. 87 (2000) 26–32.
[41] K.K. Griendling, D. Sorescu, M. Ushio-Fukai, NAD(P)H oxidase: role in cardiovascular biology and disease, Circ. Res. 86 (2000) 494–501.
[42] D.M. Okamura, J. Himmelfarb, Tipping the redox balance of oxidative stress in fibrogenic pathways in chronic kidney disease, Pediatr. Nephrol. 24 (2009) 2309–2319.
[43] E.A. Jaimes, M.S. Zhou, D.D. Pearse, L. Puzis, L. Raij, Upregulation of cortical COX-2 in salt-sensitive hypertension: role of angiotensin II and reactive oxygen species, Am. J. Physiol. Ren. Physiol. 294 (2008) F385–F392.
[44] M.J. Sullivan-Gunn, S.P. Campbell-O'Sullivan, M.J. Tisdale, P.A. Lewandowski, Decreased NADPH oxidase expression and antioxidant activity in cachectic skeletal muscle, J. Cachexia Sarcopenia Muscle 2 (2011) 181–188.
[45] M. Zhang, A. Perino, A. Ghigo, E. Hirsch, A.M. Shah, NADPH oxidases in heart failure: poachers or gamekeepers? Antioxid. Redox Signal. 18 (2013) 1024–1041.
[46] A. Nickel, J. Löffler, C. Maack, Myocardial energetics in heart failure, Basic Res. Cardiol. 108 (4) (2013) 358–362.
[47] S. Neubauer, The failing heart – an engine out of fuel, N. Engl. J. Med. 356 (11) (2007) 1140–1151.
[48]] Z. Yang, L.D. Asico, P. Yu, Z. Wang, J.E. Jones, R.K. Bai, D.R. Sibley, R.A. Felder, P.A. Jose, D5 dopamine receptor regulation of phospholipase D, Am. J. Physiol. Heart Circ. Physiol. 288 (2005) H55–H61.
[49] S. Gupta, B. Das, S. Sen, Cardiac hypertrophy: mechanisms and therapeutic opportunities, Antioxid. Redox Signal. 9 (2007) 623–652.
[50] S. Haq, G. Choukroun, H. Lim, K.M. Tymitz, F. del Monte, J. Gwathmey, L. Grazette, A. Michael, R. Hajjar, T. Force, J.D. Molkentin, Differential activation of signal transduction pathways in human hearts with hypertrophy versus advanced heart failure, Circulation 103 (2001) 670–677.
[51] J. Li, Z.H. Shao, J.T. Xie, C.Z. Wang, S. Ramachandran, J.J. Yin, H. Aung, C.Q. Li, G. Qin, T. Vanden Hoek, C.S. Yuan, The effects of ginsenoside Rb1 on JNK in oxidative injury in cardiomyocytes, Arch. Pharm. Res. 35 (2012) 1259–1267.
[52] R. Isserlin, D. Merico, R. Alikhani-Koupaei, A. Gramolini, G.D. Bader, A. Emili, Pathway analysis of dilated cardiomyopathy using global proteomic profiling and enrichment maps, Proteomics 10 (2010) 1316–1327.
[53] E.M. Jeong, M. Liu, M. Sturdy, G. Gao, S.T. Varghese, A.A. Sovari, S.C. Dudley Jr., Metabolic stress, reactive oxygen species, and arrhythmia, J. Mol. Cell. Cardiol. 52 (2012) 454–463.
[54] H. Toko, H. Takahashi, Y. Kayama, T. Oka, T. Minamino, S. Okada, S. Morimoto, D.Y. Zhan, F. Terasaki, M.E. Anderson, M. Inoue, A. Yao, R. Nagai, Y. Kitaura, T. Sasaguri, I. Komuro, Ca^{2+}/calmodulin-dependent kinase IIdelta causes heart failure by accumulation of p53 in dilated cardiomyopathy, Circulation 122 (2010) 891–899.
[55] D.J. Beuckelmann, M. Nabauer, E. Erdmann, Intracellular calcium handling in isolated ventricular myocytes from patients with terminal heart failure, Circulation 85 (1992) 1046–1055.
[56] M. Lindner, M.C. Brandt, H. Sauer, J. Hescheler, T. Bohle, D.J. Beuckelmann, Calcium sparks in human ventricular cardiomyocytes from patients with terminal heart failure, Cell Calcium 31 (2002) 175–182.
[57] W.E. Louch, V. Bito, F.R. Heinzel, R. Macianskiene, J. Vanhaecke, W. Flameng, K. Mubagwa, K.R. Sipido, Reduced synchrony of Ca^{2+} release with loss of T-tubules-a comparison to Ca^{2+} release in human failing cardiomyocytes, Cardiovasc. Res. 62 (2004) 63–73.
[58] A.N. Stammers, S.E. Susser, N.C. Hamm, M.W. Hlynsky, D.E. Kimber, D.S. Kehler, T.A. Duhamel, The regulation of sarco(endo)plasmic reticulum calcium-ATPases (SERCA), Can. J. Physiol. Pharmacol. 93 (2015) 843–854.